Dual mode transducers based on cMUTs technology

D. Gross[a], A. Boulmé[a], N. Sénégond[a], G. Férin[b], M. Legros[b], B. Roman[a], F. Teston[a] and D. Certon[a]

[a]Université François-Rabelais de Tours, 10 Bd tonnellé, 37032 Tours, France
[b]Vermon, 180 rue du Général Renault, 37038 Tours, France
dominique.gross@univ-tours.fr

More and more medical ultrasonic applications are strongly interested by the development of dual acoustic sources enable to emit high frequency ultrasound (echographic imaging) and low frequency pressure field (therapeutic ultrasounds). The use of the piezoelectricity to fabricate such device requires overcoming strong technological bottlenecks. The objective of this paper is to demonstrate that the technology of capacitive micro-machined ultrasonic transducer is able to take up this challenge. To this end a demonstrator was designed and manufactured. The first part of the paper is devoted to the design of the low and high frequency cMUTs. For the low acoustic source, a dedicated time domain model was used, taking into account the nonlinearity of the cMUT. Several simulations were conducted to optimize the emitted pressure field intensity at 1 MHz for a set of diaphragm with different sizes and geometries. The high frequency source was designed on the help of a linear model, where output parameters were central frequency, bandwidth and collapse voltage. The second part of this paper reports a set of characterization results and performances of the fabricated device: electrical impedance, mechanical displacements performed in water and acoustic pressure fields.

1   Introduction

Recent developments in targeted drug delivery have demonstrated that thermal liposomes used as drug carriers can be efficiently activated with ultrasounds [1]. Levels of acoustic intensities (typ. 1000 W/cm^2) are high but much lower than those used for High Intensity Focused Ultrasound. There is a real need today to develop dual mode transducers for these applications dedicated to small animal experiments: one function of imaging (higher than 15 MHz) and one function of therapy (lower than 2 MHz). The objective of this work is to develop such dual mode transducers based on the cMUT technology. Let's note that the development of HIFU transducers based on cMUT has already been addressed in the literature with very promising results [2]. Unlike devices presented in [3], in this work, we will demonstrate that, for our applications, High Frequency (HF) and Low Frequency (LF) cMUT can be designed with the same gap height, changing only size of membranes. One demonstrator of dual mode transducers has been fabricated and tested. The manufacturing procedure was a LPCVD-based sacrificial release process.

2   Design aspect of dual mode transducer

2.1   Geometrical configuration

The dual mode transducer we aimed to develop is composed of three linear arrays: one for high frequency imaging (15 MHz) and two for therapeutic applications (lower than 2 MHz). The total dimension of the transducer has to be small enough to be compatible with small animal imaging. The high frequency array is made of 128 elements with a pitch of 125 µm, whereas each low frequency array consists of 32 elements with a pitch of 500 µm. Furthermore, a mechanical focusing is required in addition to an electronic focusing to provide enough pressure field amplitude for therapeutic applications. Then, an acoustic lens (Figure 1 – right) is placed at the front of the transducer in order that the low frequency and the high frequency arrays emit ultrasound in the same plane. With this configuration, we can expect, in the [1 MHz – 2 MHz] range, a gain of 100 between the spatial peak pulse average intensity (I_{sppa}) at the focus point and the one radiated at the surface of the array. The useful working distance for the therapeutic and imaging arrays is fixed to 15 mm.
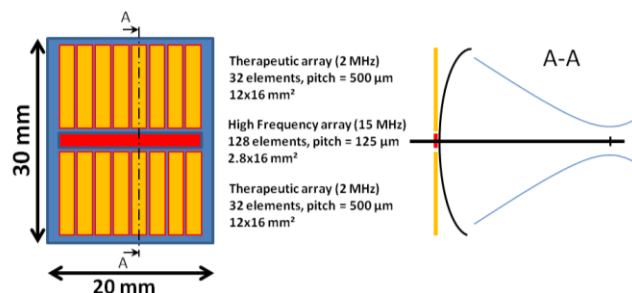

Figure 1: Geometrical configuration of the transducer

The design of the two kinds of membranes must fulfil some common requirements:

- The difference in size of HF and BF membranes has not to be too strong in order that the time etching of the two populations of cavities, during the micromachining process, be similar,
- The same gap height,
- The gap has to be small enough in order that the collapse voltage for the HF membranes does not exceed 200 Volts (safety and electric insulation),
- The gap has to be large enough to maximize the emitted low frequency acoustic power.

2.2   Design of the membranes

A simulation has been conducted to take into account all trade-offs and design rules that involve those requirements. The membrane is made of SiN material (Table 1) covered with an aluminum electrode (surface ratio of 50%). The gap height was fixed to h_{gap} = 200nm. To simplify simulations, we considered that the cMUT cells were square with a 2D periodic layout. The distance between membranes was 7 µm. The model described in [4] was used for simulations. Three master curves are required to choose the size of membranes. The two first (Figure 2) are the variations of the central frequency and the collapse voltage against the size of the membrane.

Table 1: Dimensions of cMUT membranes and physical properties of material used for simulation.

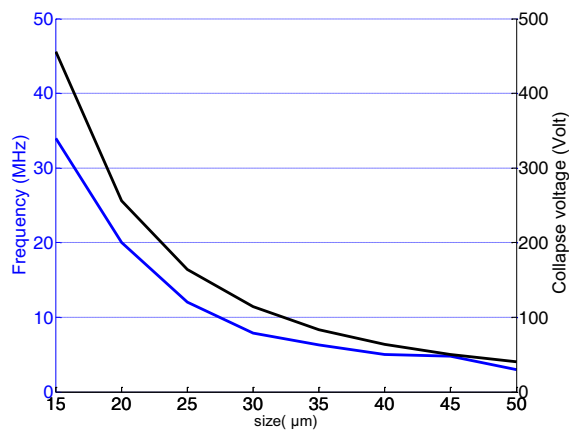| Layer	SiN	Al
Thickness (nm)	600	450
E (GPa)	220	E_e = 68
σ	0.24	0.35
ρ (kg/m^3)	3300	2700
ε_r	7.5	

Figure 2 : Variations of central frequency (blue) and collapse voltage (black) against size of membranes.

The analysis of the Figure 2 points out an interesting range of widths for the HF design: from 20 to 25 μm. The central frequency goes from 15 MHz to 20 MHz and the collapse voltage does not exceed 200 Volts.

In the case of LF array, we clearly observe that to decrease the central frequency to 2 MHz, a large surface membrane is required. But the selection of the cMUT design is more difficult, because of some fabrication issues with such membranes: with micromachining process, The etching time is very long and the membranes could be stuck at the back of the cavity during excavation. More, since cavities are sealed under vacuum, the atmospheric pressure strongly deflects large membranes. For example, with a size of 50×50 μm^2, the deflection is 70 nm.

To overcome such risk of membrane deterioration, we can choose to optimize BF membranes in order to force their vibrations at frequency lower than their central frequency. In a previous study [5], it has been clearly demonstrated that, for a membrane with central frequency f_c, thanks to non-linearities of electrostatic forces, the amplitude of an excitation voltage close to Vc/2 is high enough to produce a spatial peak-to-peak displacement amplitude equals to the half of the cavity depth. To optimize the size of BF membranes, we can so assume that the spatial maximum of displacement amplitude is equal to:

$$u_0 = \left(hgap - deF \right) \div 2 \qquad (1)$$

Where deF is the static deflection of the membrane caused by atmospheric pressure. The radiation impedance R_a of the transducer, for 2D periodic layout, is equal to the fluid acoustic impedance multiplied by the surface coverage ratio. Knowing u_0 and R_a, the radiated mean acoustic intensity is easy to compute as followed:

$$P_a = \frac{1}{2} R_a \left(2\pi f_0 \frac{u_0}{3} \right)^2 \qquad (2)$$

f_0 is the excitation frequency and u_0 is divided by 3 to obtain the mean spatial displacement amplitude over the membrane.

The second master curve is the variations of P_a against the size of the membrane (Figure 3). The optimization of

the output acoustic intensity for therapeutic arrays is a trade-off between a large membrane size for which amplitude displacement is reduced but R_a value is high and small membrane size, for which the amplitude displacement is strong but the radiation impedance is small.

For this example of design, the optimum membrane size was 30 μm, where at the surface of the transducer, the I_{sppa} value reaches 8 W/cm^2 at 2 MHz.
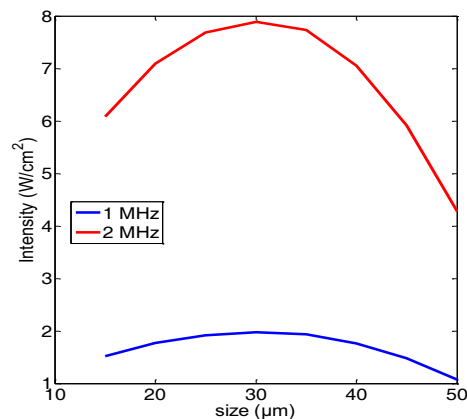

Figure 3 : Variations of the spatial peak pulse average intensity against the size of the membrane for 1 MHz and 2 MHz CW excitation frequencies.

To estimate the focusing gain and the size of the focal spot, the acoustic field pressure radiated by the two low frequency arrays taking into account the lens was simulated using the Matlab$^®$ DREAM toolbox [6]. Each element are made with the predetermined optimum membrane size of 30x30 μm² and the mean displacement amplitude. Each acoustic source was excited with one cycle of sinusoid centered at 1 MHz and 2 MHz, and the mean spatial displacement over the membranes was determined thanks to equation 1. The latter has been computed taking into account a static deflection of the membrane of 9 nm.

The maximum pressure level at the focal point is 2 MPa at 1 MHz (Figure 4), while it reaches about 4 MPa at 2 MHz.
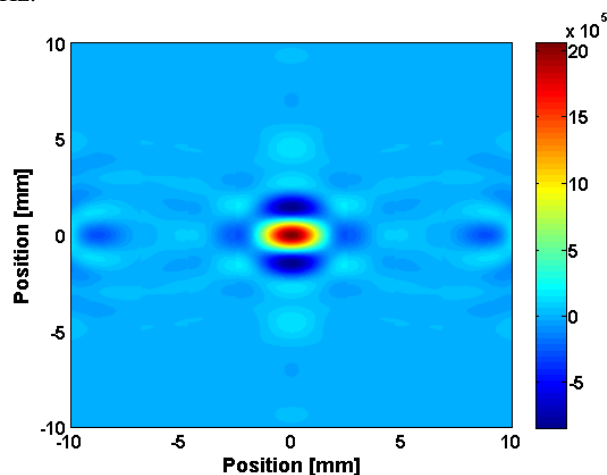

Figure 4: Pressure field at the focal plane [Pa]

From these results, the spatial peak pulse average intensity was computed (Figure 5). Note that, in this case, it is computed peak pressure intensity. The maximum

intensity reaches, at the focal point, 154 W/cm² and 534 W/cm² at 1 MHz and 2 MHz respectively.
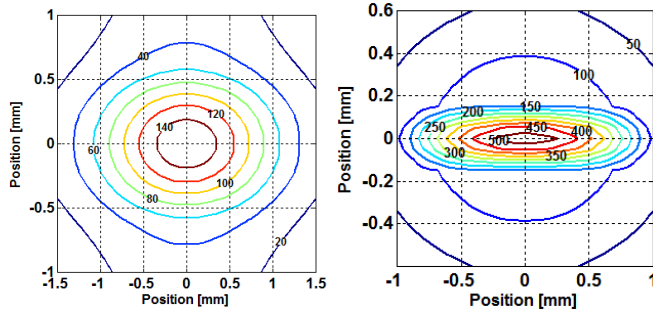

Figure 5: Spatial Peak Pulse Average Intensity [W/cm²], at 1 MHz (left) and 2 MHz (right).

This computation allows the determination of the focusing gain. By dividing the intensity at the focal spot by the one of the excitation, we obtain a gain about 120 in this configuration.

These results show that such a probe design can reach sufficient pressure levels at the region of interest for therapeutic applications.

3   Method: Fabricated devices

To experiment and test performances of dual mode transducers with single gap, HF and BF array prototypes were fabricated, on the same wafer, with LPCVD micromachining process described in [7].

The details of the membrane configuration are given for each array (Table 2). Here, rectangular shape membranes were chosen in order to increase the active acoustic surface ratio. However, the aspect ratio of each rectangle is inferior to 2 to avoid the presence of spurious resonance modes of rectangular membranes in the response of the array.

Table 2: Geometry and material properties of manufactured HF and BF cMUTs.

Geometry of membranes			Materiel Properties		
	BF	HF	Layer	SiN	Al
Size	60*30	27*20	Thick. (nm)	650	450
kerf (µm)	10	10	E (GPa)	220	$E_e = 68$
H_{GAP}	200	200	σ	0.24	0.35
V_c (Th)	77 V	212 V	ρ (kg/m³)	3150	2700
V_c (Exp)	70 V	210 V	ε_r	9.5	

For each configuration, the length of the small size of membranes was defined in accordance with previous simulations. The first characterization step was the measurement of the static collapse/snapback cycle with Digital Holographic Microscope (Figure 6) and the electrical impedance (Figure 7). The experimental collapse voltages were respectively 210 V (HF) and 77 V (LF). The theoretical values are given in Table 2. They are well predicted as the electrical impedance, which validates our input data of model.
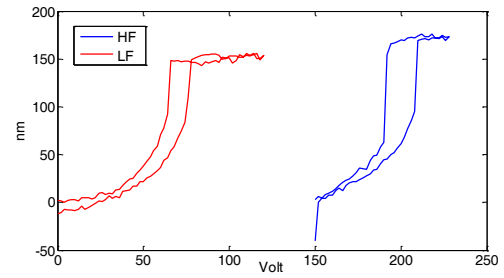

Figure 6: Experimental collapse/snapback cycle measured for the HF and LF membranes.

The theoretical pressure spectrum was computed for each array (Figure 8). We see that the central frequency of the spectrum is different than the position of the maximum value of electrical impedance. The spectrum is shifted toward higher frequencies. The therapeutic array pressure spectrum was centered at 5 MHz and 15 MHz for the HF imaging array. At this step of our development, in order to facilitate evaluation of HF and LF array performances, the two devices were individually integrated and electrically connected onto a PCB.
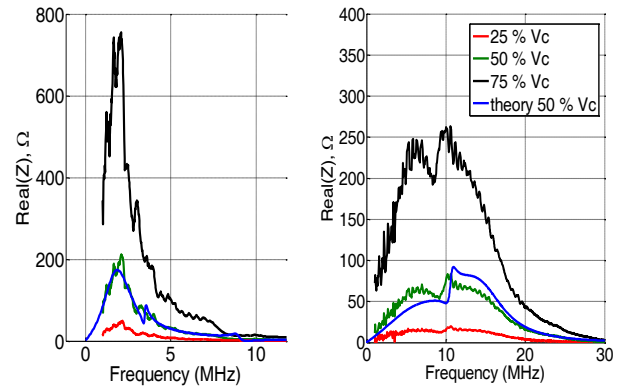

Figure 7: Electrical impedance – real part of one element of array loaded with oil for different biasing voltage values. Left : LF array and right : HF array.
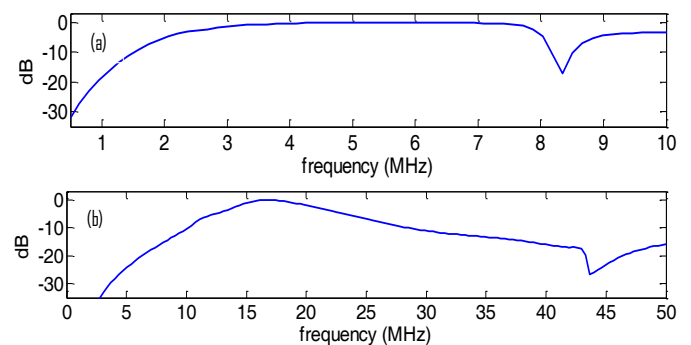

Figure 8: Theoretical pressure spectrum emitted by LF (a) and HF (b) arrays.

Each prototype has been covered with a 500 µm silicone layer. Their performances were evaluated by measuring, with a laser interferometer (Bossa Nova– 30 µm laser spot size - Figure 9), the mechanical displacements produced at the front face of the transducer.
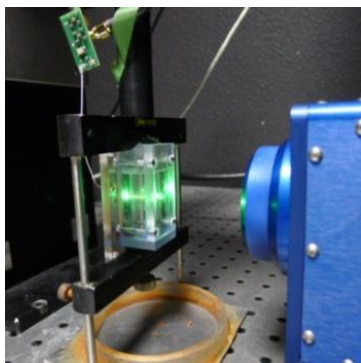
Figure 9: Setup of the displacement measurement with laser interferometer.

4   Results : High frequency array performances

The high frequency device has been characterized as a standard linear array. A single element was electrically excited with one cycle of sinusoid centered at 20 MHz, with peak to peak amplitude of 50 V. The electronic emitter was a waveform generator coupled with a large bandwidth amplifier. The bias voltage was 180 V. The displacements were scanned along the array over a 2 mm width and a pitch of 15 μm. A second scan along the elevation was performed to determine the height of the acoustic aperture at the surface of the array. 2.8 mm was measured, that was in agreement with the geometry of the element.

From the scan of the displacement, pressure field properties radiated by one element are easy to determine using standard acoustic tools based on the Rayleigh integral formulation. In our case, we used the DREAM software. The results are reported in Figure 10. The performances are close to the expected ones. We measured a peak-to-peak magnitude of displacement of 2.5 nm, which is a significant value for this frequency range of working. The pulse pressure confirms this aspect with a peak-to-peak pressure of 160 kPa measured at 2 mm away from the transducer. Looking at the corresponding spectrum (Figure 10 d.), we observe that the central frequency (13 MHz) and the bandwidth (the -6 dB fractional bandwidth is 95 %) are smaller than the targeted value. This one originates from two reasons: the presence of the silicone layer strongly attenuates high frequency ultrasound.

Note that the compensation of the silicone attenuation (Figure 10 d.) shifts toward higher frequencies the bandwidth but it remains lower than the theory. The second reason comes from the electronic waveform generator. Its practical maximum frequency bandwidth was 25 MHz, although the technical specifications of the apparatus allow emitting pulse centered at 20 MHz.

This second aspect is a key point of the excitation of high frequency cMUT arrays that will be addressed in future works. Finally, the polar directivity, i.e. the peak-to-peak time pressure amplitude against radiation angle, was computed (Figure 10 b.). As for all cMUT arrays, this device shows a high value of directivity: ±35° at -6 dB from the maximum.
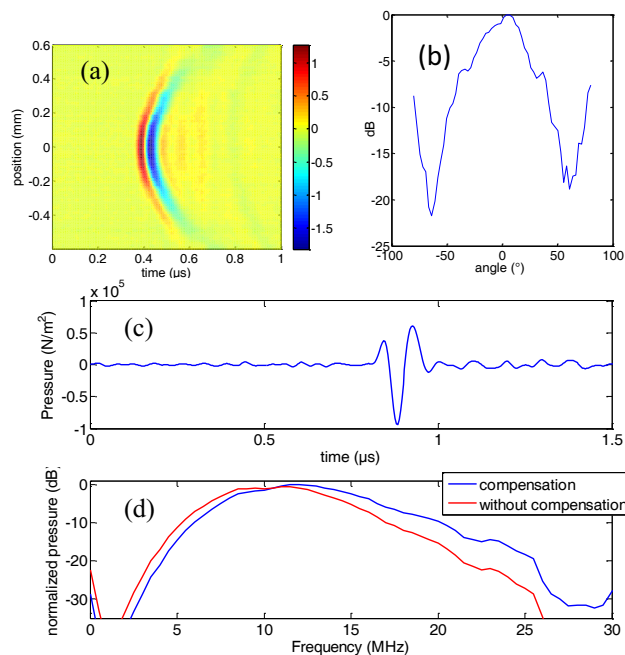

Figure 10: Characterization results of the High frequency array. (a) Scan of the displacement. (b) peak to peak directivity of the pressure field. (c) Pulse pressure emitted at 2 mm in the axe of the element. (d) spectrum of the pulse pressure.

5   Results: therapeutic array performances

The LF frequency array was tested in order to measure its ability to radiate strong intensity ultrasounds at 1 MHz and 2 MHz. As explained in the second paragraph, the best conditions of the electrical excitation were looked for producing the strongest displacement amplitudes. For that, cMUTs had to vibrate in "dynamic collapse/snapback" mode in order that the maximum peak-to-peak displacement amplitude being equals to the h_{GAP} value. The determination of the output acoustic intensity requires knowing, at each point of the transducer surface, the pressure and the particular velocity fields both. Obviously, if the acoustic aperture is large comparing with the acoustic wavelengths, the ratio between the pressure field and the particular velocity is locally equal to the impedance of the fluid. The first objective of our experiments had to verify these conditions. For that, one element was electrically excited with a single sinusoidal pulse centered respectively at 1 MHz and 2 MHz (50 V_{pp}) and a 60 V bias voltage. A scan was performed along the array and along the elevation. For the two frequencies, the exact pressure field, computed with all the displacement field, was the same than the estimated one, computed only with the local particular velocity field response (× 1.5 MRayls) (Figure 12). The estimation of the maximum spatial peak pulse average intensity is easy to derive numerically from the spatial maximum of the displacement.
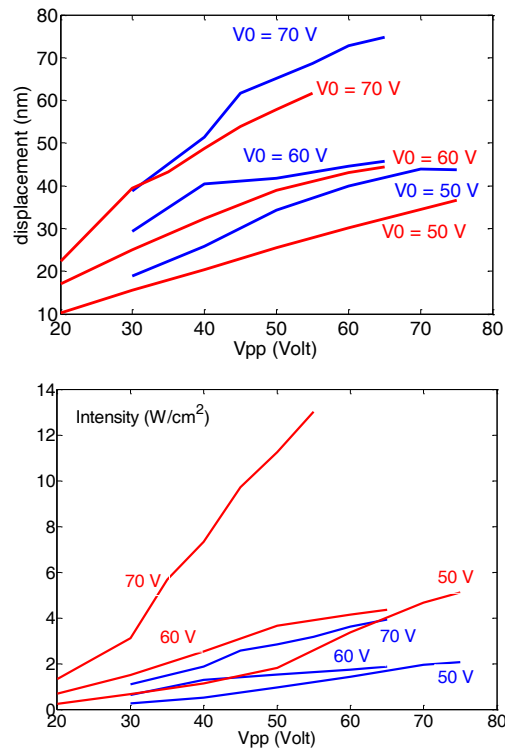
Figure 11: Peak to peak displacement (nm) and intensity I_{sppa} measured at the front of the transducer for one pulse of 1 MHz and 2 MHz for different polarization and voltage amplitude.

The second objective of experiments was to define the best conditions for which the displacement amplitude and intensity I_{sppa} at the surface of the transducer were maxima. For that, we kept the excitation conditions, and modified the bias voltage (V_0) and the amplitude of excitation voltage (V_{pp}). The results are reported in Figure 11. As expected, the amplitude and the intensity increase with the bias voltage and the excitation voltage amplitude. We note that the strongest displacements are obtained at 1 MHz. The membranes work in "dynamic collapse/snapback" mode for which the dynamic collapse value is lower at 1 MHz than at 2 MHz. Then, at 1 MHz, with the same voltage, the mean displacement swept by the diaphragm will of course be higher. However, when we look at the intensity, the strongest values are obviously reached at 2 MHz. With a transducer with a focusing gain of 100, we see that values of 400 W/cm^2 can be obtained at 1 MHz and 2 MHz. The maximum is close to 1200 W/cm^2, at 2 MHz, for V_0=70 V and V_{pp}=50 V. Finally, we have tested at 1 and 2 MHz the stability of the cMUTs response versus time for very long CW excitations, like the ones used in HIFU protocols (Figure 12). The performances of cMUTs are clearly demonstrated here. At 1 MHz, even if intensity values are lower than the thermal activation of liposomes required, the stability of the response confirms that cMUT are a very good candidate for therapeutic applications. Obviously, the lack of intensity can be compensated by either an increase of the transducer surface,or an increase of the gap. At 2 MHz, high values of intensities are confirmed. It seems that the acoustic power slightly decreases with time. However, this phenomenon is not enough significant here to bring conclusions about the origins of these variations. These results have to be confirmed with other experiments.
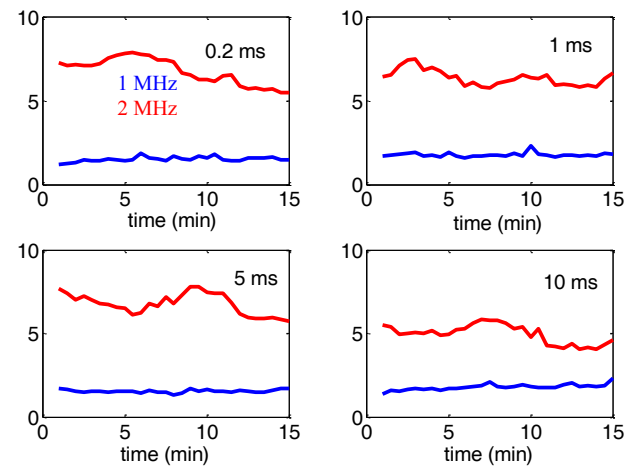

Figure 12: Pulse Peak Time Average Intensity (W/cm^2) measured for long CW excitation versus time. Duty cycle is 50 % and burst period 0.2, 1, 5 and 10 ms. V_0 = 70 V, V_{pp} = 60 V.

6   Conclusion

The concept of dual mode cMUT with single gap is validated in this work. Two arrays, one for high frequency imaging and another for therapeutic applications, were designed and manufactured with promising performances for targeted drug delivery applications. However, for small animal experiments, it seems essential to work at 2 MHz to maintain integrated small size transducer. The subjects of future works are to improve the HF array protection layer, finish the integration of the transducers and test it in real conditions.

Acknowledgment

References

[1]   D. Chen, "Applications of acoustic techniques to targeting drugs delivery and dust removal relevant to nasa project" Ph. D. thesis, University of Vermont, 2010.

[2]   S. H. Wong et al., "Feasibility of MR-Temperature Mapping of Ultrasonic Heating from a CMUT," *IEEE UFFC*, vol. 55, no. 4, pp. 811-817, Apr. 2008.

[3]   M. Wang et al., "Design and Test of a Monolithic Ultrasound-Image-guided HIFU Device using Annular CMUT Rings," in *Proceedings of IEEE International Ultrasonics Symposium*, 2008, pp. 459-462.

[4]   C. Meynier et al, "A multiscale model for arrays of capacitive micromachined ultrasonic transducers," *Journal of Acoustical Society of America*, vol. 128, no. 2, pp. 2540-2561, Dec. 2010.

[5]   N. Sénégond, "Time domain approach to model and characterize capacitive micromachined ultrasonic transducers," Ph. D. Thesis, François-Rabelais University, Tours, 2010.

[6]   F. Lingvall. http://www.signal.uu.se/Toolbox/dream/.

[7]   E. Jeanne, "Fabrication and characterization of capacitive micromachined ultrasonic transducers," Ph.D. thesis, François-Rabelais University, Tours, 2008.